Progress in Oceanography xxx (xxxx) xxx–xxx

Contents lists available at ScienceDirect

Progress in Oceanography

journal homepage: www.elsevier.com/locate/pocean

Death in southern Patagonian fjords: Copepod community structure and mortality in land- and marine-terminating glacier-fjord systems

R. Giesecke[a,b,*], J. Höfer[a,b], T. Vallejos[a,c], H.E. González[a,b]

[a] Instituto de Ciencias Marinas y Limnológicas, Universidad Austral de Chile, Independencia 631, Valdivia, Chile
[b] Centro FONDAP de Investigación en Dinámica de Ecosistemas Marinos de Altas Latitudes (IDEAL), Valdivia, Chile
[c] Programa Magister en Recursos Hídricos, Universidad Austral de Chile, Chile

ARTICLE INFO

Keywords:
Copepod carcasses
Swimmers
Vertical carbon flux
Magellan Region
Freshening

ABSTRACT

Glacial retreat at high latitudes has increased significantly in recent decades associated with global warming. Along Chile's Patagonian fjords, this has promoted increases in freshwater discharge, vertical stratification, and the input of organic and inorganic particles to fjords. In addition, it has modified the water chemistry [i. e. nutrient stoichiometry] and its associated biota. This study evaluates the effect of deglaciation in high-latitude fjords (54°S) on copepod survival and how this might affect the export of particulate organic carbon to the benthos. We selected two contrasting fjord systems in terms of their geomorphology and the quality and quantity of freshwater contributions: (a) Pia Fjord, with marine-terminating glaciers, and (b) Yendegaia Fjord, with land-terminating-glaciers. Both are located along the Beagle Channel (54°S), southern Chilean Patagonia.

These two fjords differed significantly in phytoplankton and copepod biomass. Whereas Pia Fjord showed high chlorophyll-a concentration (7 mg Chl-a m^{-3}) and copepod abundance (970 ind. m^{-3}), in Yendegaia Fjord, the biomass was very low for both autotrophs (< 0.3 Chl-a m^{-3}) and copepods (470 ind. m^{-3}). Conversely, a greater proportion of copepod carcasses was recorded in Pia (22%) versus Yendegaia (18%), with small copepods (600–1000 μm prosome length) being less affected than large ones (> 1000 μm). The presence of carcasses was better explained by the amount of suspended particulate inorganic matter in the water column than by salinity. The contribution of dead copepods to the vertical carbon flux was < 3.5% of the total carbon exported down to 50 m depth, with contributions of 9.5 ± 9.9 mgC m^{-2} d^{-1} in Yendegaia and 10.8 ± 10.8 mgC m^{-2} d^{-1} in Pia. Our results suggest that heavy deglaciation processes in high-latitude fjords may reduce phytoplankton biomass, causing the copepod abundance to decrease and non-predatory mortality in filter-feeding copepods to decline.

1. Introduction

The retreat of glaciers at high latitudes has increased due to the rise of global temperatures. Increased melting has promoted accelerated freshwater runoff to the ocean (Dyurgerov et al., 2010), decreases of sea surface salinity and light penetration, increase of vertical stratification and sediment runoff in coastal areas. The magnitude and structure of these processes are closely related to the type of connection between glaciers and marine systems. Land-terminating glaciers discharge suspended sediments from glacier erosion, and meltwater runoff transports these sediments to the ocean. This brackish water, which is loaded with fine sediments, is projected into the fjords as a narrow buoyant plume (Chu, 2014). The plume affects both the structure of the water column (via increased vertical stratification) and light penetration (via increased turbidity of surface waters). In the case of marine-terminating glaciers, part of the metlwater comes from the surface of the glacier, while meltwater is also released bellow the sea surface, generating an upwelling of deep sediment and nutrient rich water (basal meltwater) (Murray et al., 2015; Meire et al., 2017). Given the lower density of the basal meltwater, it rises to the surface and produces a shallow surface turbidity plume that penetrates into the fjords (Cuffey and Paterson, 2010). These plumes impinge on the system such that the plume's high turbidity and low salinity are distributed over a wider depth stratum while remaining near the glacier (Straneo et al., 2011).

The consequences of these distinct types of runoff on the biological productivity of high-latitude coastal and fjord ecosystems have just recently been addressed (e.g., Meire et al., 2017). Glacier runoff may provide inorganic (nutrients) and organic matter (dissolved and particulate) during the melt season (Bhatia et al., 2013; Hawkings et al., 2015; Wadham et al., 2016), resulting in highly unbalanced nutrient

* Corresponding author at: Instituto de Ciencias Marinas y Limnológicas, Universidad Austral de Chile, Independencia 631, Valdivia, Chile.
E-mail address: ricardo.giesecke@uach.cl (R. Giesecke).

https://doi.org/10.1016/j.pocean.2018.10.011

stoichiometry (Meire et al., 2016). In the case of Chilean Patagonian rivers, this imbalance seems to respond to an uneven influx of high amounts of silicic acid and low nitrate and phosphate concentrations (González et al., 2011, 2013). Moreover, a recent study has shown that, in Greenland, ecosystem productivity for marine-terminating glaciers is higher than for land-terminating glaciers due to the upwelling of subsurface melt-water plumes (Meire et al., 2017).

With the ongoing melting of high-latitude ice fields, marine-terminating glaciers are retreating and will ultimately be transformed into land-terminating glaciers. Marine-terminating glaciers are more sensitive to changes in air temperature than river-fed fjords (Chu et al., 2009). The number of studies analyzing the impacts on the productivity and pelagic structure of adjacent marine ecosystems have increased over the last decades. However, the potential positive or negative impacts on the pelagic ecosystem functioning are still poorly known.

Copepods are the most abundant metazoans in aquatic ecosystems and represent an important link between primary producers and higher trophic levels, playing a key role in marine food webs and biogeochemical cycles (Verity and Smetacek, 1996). Copepods play a significant role in the fate of organic matter and the amount of material exported from the pelagic realm to the benthos (Turner, 2002). In the last decade, there has been an increasing interest in studying the effect of melting glaciers on copepod grazing (Tang et al., 2011; Arendt et al., 2011, 2016), copepod distribution (Weydmann and Kwasniewski, 2008) and community structure (Arendt et al., 2016). However, how marine- and land-terminating glaciers will affect copepod survival and their impacts on copepod community structure have not been addressed yet.

The Cordillera Darwin Icefield (CDI), part of the southernmost Sub-Antarctic glacier relicts, constitutes the third largest temperate icefield in the Southern Hemisphere, after the North and South icefields of Patagonia (Bown et al., 2014). The Beagle Channel, which delimits the south-west border of the CDI, receives freshwater discharges directly or through adjacent fjords. Most of these fjords are directly influenced by a glacier, and only a few have land-terminating-glaciers.

This study evaluates the copepod community structure, carcass abundances in the upper 50 m water column, and copepod contributions to vertical carbon and nitrogen fluxes along two distinct fjords: one with land-terminating-glaciers (Yendegaia Fjord) and one with marine-terminating glaciers (Pia Fjord). The possible causes of copepod mortality are also discussed in terms of the physical, chemical, and biological characteristics of these two geomorphologically different fjords.

2. Materials and methods

2.1. Oceanographic information

Hydrographical data from two fjord systems were collected during a cruise in October 2016. A CTD Seabird 19plus was deployed from the surface down to a few meters above the bottom along a transect in each fjord. Chlorophyll-a (Chl-a) concentrations and water column transmittance were recorded with a fluorometer (FluoroProbe BBE, Moldaenke) within the upper 50 m. At each station (Fig. 1), discrete water samples were collected using a 5-L Go-Flo oceanographic bottle at various depths: 0, 5, 10, 15, 25, and 50 m. Two subsamples (250 ml each) were filtered through pre-combusted and weighted Whatman GF/F filters in order to estimate inorganic matter concentrations using the gravimetric method (Banse et al., 1963). Subsamples (200–300 ml) for measuring Chl-a concentrations (duplicate) were filtered through Whatman GF/F filters and frozen immediately at −20 °C. At the laboratory, Chl-a was extracted in 90% acetone under dark conditions (Parsons et al., 1984) and measured with a Turner Designs TD-700 fluorometer.

2.2. Copepod sampling and carcass identification

Zooplankton samples were collected at three stations along each fjord (Fig. 1) by means of oblique hauls using a bongo net (50 cm net diameter, 200 µm mesh size) towed from 150 m depth to the surface. The net was equipped with a Hyrdo-Bios calibrated flow-meter. We used the neutral red staining method to determine dead and live zooplankton (Dressel et al., 1972; Elliott and Tang, 2009). Freshly caught zooplankton were gently transferred from the cod-end to a plastic jar, and 4 ml of neutral red stain (1:1000) were added per 100 ml of sample. Zooplankton were stained for 10 min before being preserved in a 5% formaldehyde seawater solution buffered with sodium acetate. Samples were stored for no more than two months in dark and cold prior to analysis. Also prior to analysis, samples were acidified with acetic acid to pH < 7 to develop the stain color. Zooplankton were identified, counted, and classified as dead or alive using a Nikon SMZ1000 stereomicroscope with C-DSC diascopic illumination, as suggested by Elliott and Tang (2009). Copepodite stages CI to CIII were not indentified to species level and therefore were grouped into “copepodites”. Samples had to be analysed rapidly to avoid stain fading after acidification (Elliott and Tang, 2009), so we had to optimize the time used for identification, to stages which were easy to identify down to species or genus level.

The percentage of carcasses was studied by linear regression and model selection using the proportion of dead copepods as the response variable. Before running the linear regression analysis, our response variable (i.e., proportion of dead copepods) was transformed by the arcsine of the square-root, which is applied when a variable is a proportion or percentage (Underwood, 1997). Using second-order Akaike Information Criteria (AICc) for model selection allowed us to test two hypotheses: the “osmotic” hypothesis, in which copepod mortality was more likely caused by low salinities, and the “clogging” hypothesis, in which mortality is due more to feeding/gut disruptions from high amounts of inorganic suspended matter in the water. Functions lm (package stats) and aictab (package AICcmodavg) were used for linear regressions and model selection using R version 3.1.0 (R Core Team, 2012), respectively.

2.3. Sediment traps

Vertical fluxes of particulate organic carbon (POC) and nitrogen (PON) were estimated by deploying two quadruple cylindrical sediment traps (capture area: 50 cm^2, aspect ratio: 8.3) in each fjord, one close to the fjord head and the other at the fjord mouth. The traps were installed at 50 m depth for 24–51 hrs over bottom depths of 120–150 m. Because of the short deployment time, no preservatives were added to the collection cups (Ivory et al., 2014). Prior to deployment, the traps were filled with filtered seawater (0.7 µm pore size) and one cylinder was filled with 7.5 mg L^{-1} neutral red (NR) to stain the copepods. This allowed us to distinguish between copepod swimmers and carcasses (Ivory et al., 2014). After retrieval, the collecting cup stained with NR was fixed in a 5% formaldehyde seawater solution buffered with sodium acetate. These samples were later analyzed under a Nikon SMZ1000 stereomicroscope to identify, count, and classify (i.e., dead/alive) copepods. Water samples from the two remaining sediment trap cups were pre-screened through a 200-µm sieve, to avoid overestimating the vertical carbon flux due to the presence of swimmers. For the quantification of particulate organic carbon and nitrogen (POC and PON) fluxes, sub-samples (20–50 ml, three replicates) were filtered through pre-combusted, 0.7-µm GFF filters and immediately frozen at −20 °C until later elemental analysis at the stable isotope facility of UC-Davis (California).

2.4. Copepod contributions to carbon and nitrogen vertical fluxes

Live copepods and carcasses retained in the stained sediment trap

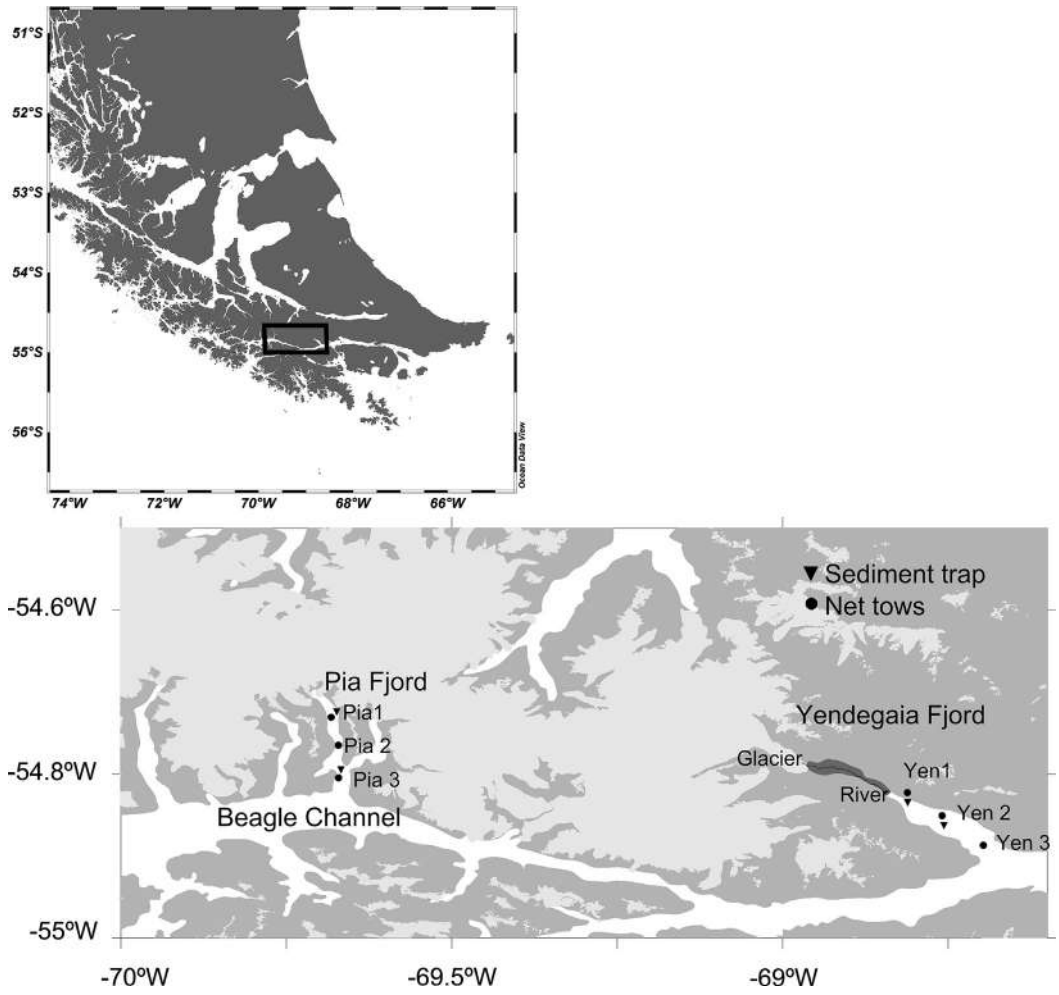

Fig. 1. Map of the study area with sampling stations. Black circles show stations including, water column sampling, and net tows. CTD and fluoroprobe casts were done on a higher spatial resolution along the fjord. Triangles indicate the location of sediment traps. Light grey area show the Cordillera Darwin Icefield field location. Dark grey area at the Yendegaia fjord represent the river basin.

samples (see above) were identified up to the species level and measured (prosome length, PL, in μm). Carbon and nitrogen weights were estimated for carcasses and swimmers using a length-weight regression for each copepod species/genus (Supplementary material Table 1). Carbon and nitrogen losses from carcasses due to microbial degradation were assessed using a temperature-dependent degradation rate (Elliott et al., 2010). Copepod carbon and nitrogen fluxes were standardized to a 24-hr period in order to obtain the daily flux of carcasses and swimmers per square meter per day. The same procedure was used for total POC and PON fluxes.

For each sediment trap, we analyzed which copepod species were actively swimming into the traps and which were reaching the traps already dead. To discriminate, we applied an adapted version of the selectivity index E (Ivlev, 1961); $E = (ri - pi)/(ri + pi)$, where *ri* is the proportion of carcasses belonging to taxon "*i*" and *pi* is the proportion of swimmers of that same taxon in the same sediment trap. Negative values indicate a greater proportion of copepod swimmers, whereas positive values represent a greater proportion of dead copepods.

2.5. Influence of environmental parameters on copepod species composition

The relationships between copepod abundances (all taxa separately) and environmental variables were analyzed using redundancy analysis (RDA). RDA is a constrained ordination, which, using linear combination of explanatory variables, looks for the orthogonal axes that best explain response variables (see details in Borcard et al., 2011). Essentially, RDA is a multi-response, multiple linear regression followed by a principal component analysis (PCA). Mean values, down to 50 m depth, of inorganic matter, organic matter, temperature, salinity, and Chl-a concentrations (log transformed) were used as explanatory variables. Linear regression is sensitive to co-linearity among explanatory variables. Therefore, we obtained a correlation matrix for our explanatory variables and chose the three variables (inorganic matter, salinity, Chl-a concentration) presenting the weakest correlations (Pearson's $r < 0.45$), following suggestions to use only explanatory variables with correlation coefficients < 0.75 (Ayata et al., 2011). RDA was performed using the *rda* function from the *vegan* package. RDA site scores were estimated as a weighted sum of species, since this procedure is more robust to noise in environmental variables (McCune, 1997). Significance of RDA axes was assessed by a permutation test (1000 iterations) using the *anova.cca* function from the *vegan* package. Permutation solves the problems caused by non-normal distributions in testing RDA significance (Borcard et al., 2011). All copepod abundances were logarithmically transformed before analysis.

Abundances of all copepod taxa were analyzed using a variation partitioning method based on successive partial linear regressions (Borcard et al., 1992; Legendre and Legendre, 1998) improved using adjusted R^2 estimations (Peres-Neto et al., 2006). Only three explanatory variables (inorganic matter, salinity, Chl-a concentration) were used to reduce their co-linearity (see above). Variation partitioning allows us to know which fraction of the variance is solely explained by each variable and which fraction is jointly explained by two

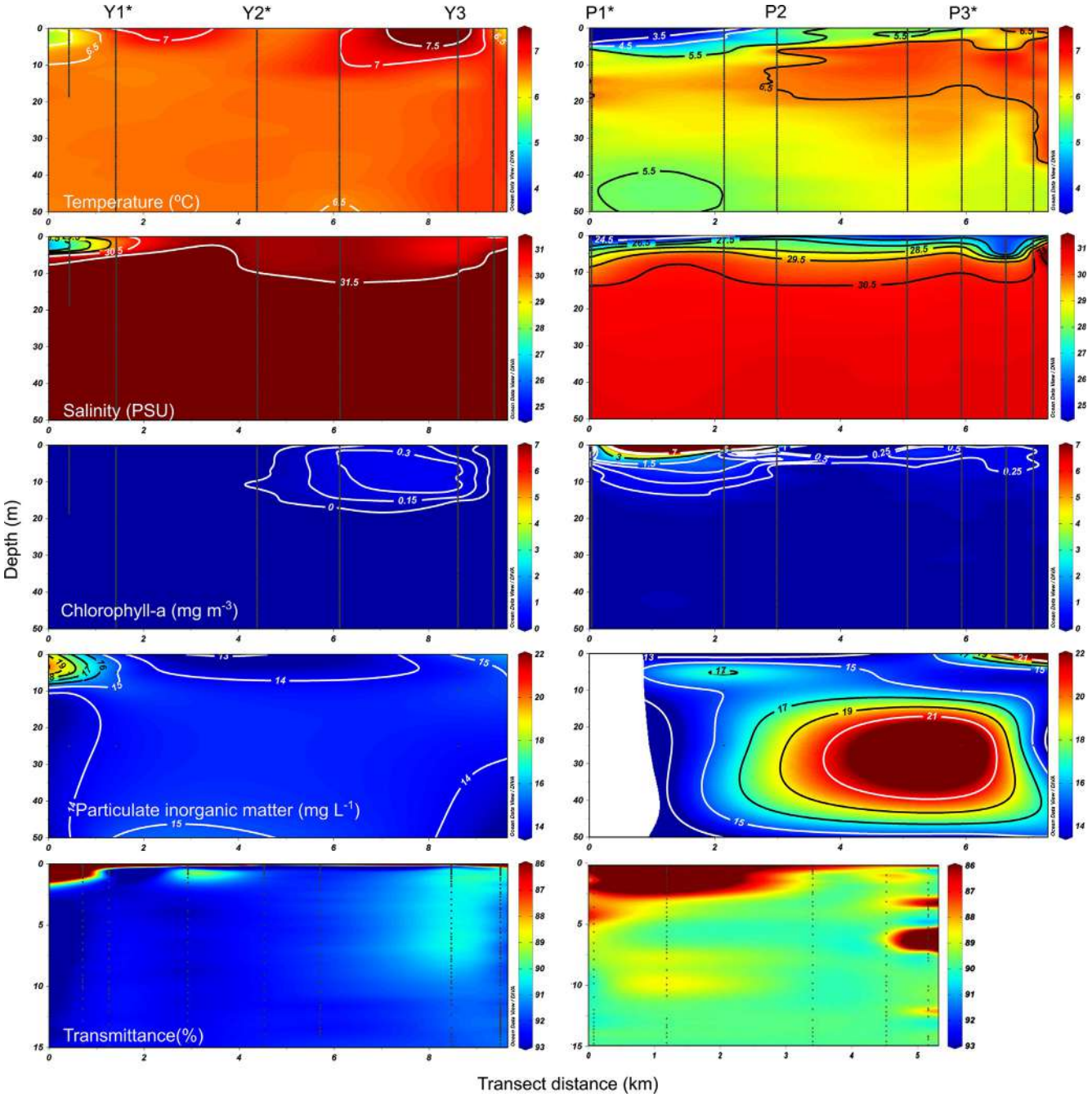

Fig. 2. Vertical distribution of physical, chemical, and biological variables recorded along both fjords following the transects shown in Fig. 1 (left: Yendegaia Fjord, right: Pia Fjord). The panels show the distributions of temperature (°C), salinity (PSU), Chlorophyll-a (mg m^{-3}), suspended particulate inorganic matter (mg L^{-1}), and transmittance (%).

or three variables. A subtractive procedure was used to produce unbiased estimations of the fractions of variation explained (see details in: Peres-Neto et al., 2006; Borcard et al., 2011). The variation partitioning was performed using the *varpart* function from the *vegan* package following recommendations by Borcard et al. (2011).

3. Results

3.1. Oceanographic information

There was a clear difference in water column structure along the two studied fjords in October 2016. Yendegaia Fjord (YF) presented a cooler (6 °C), more homogeneous water column with slightly lower salinity (27 psu) near the meltwater plume than at the fjord mouth (31 psu), inducing stratification in the upper 10 m along the fjord (Fig. 2). Chlorophyll-a concentrations were low along the entire fjord, especially at the head (< 0.1 μg L^{-1}), where the upper water column was heavily influenced by meltwater discharge, and increasing slightly (up to 0.3 μg L^{-1}) near the mouth. Surface meltwater input was characterized by high levels of inorganic matter and turbidity; this was observed in only a thin layer (upper 20 cm) along the entire fjord (Fig. 2). Therefore, the higher inorganic matter concentrations registered close to the fjord head decreased drastically with salinity.

Pía Fjord (PF) showed considerably higher meltwater input and lower salinity and temperature than YF along the whole water column, with a conspicuous low salinity plume and stratification within the

upper 10 m along the entire fjord. The melting of icebergs calved from marine-terminating glaciers diminished surface water temperature (< 3°C) and salinity (24 psu), while promoting high Chl-a concentrations (up to 7 μg L^{-1}) above the thermocline; these decreased from the glacier to the fjord mouth (Fig. 2). Inorganic suspended matter (ISM) inputs brought by glacier meltwater from the surface and underground (water that percolates down the glacier, entering the fjord at depth) increased water turbidity along the whole fjord and the entire water column, reaching levels up to 22 mg L^{-1} (Fig. 2).

Stations close to freshwater discharges showed less similarity between them and among them and the other stations within each fjord (Fig. 5a). These differences were mainly caused by Chl-a concentrations (highest values in PF and lowest in YF) and ISM concentrations (low in YF) and salinity (low in PF). Properties (Chl-a, salinity, ISM) at stations located at the middle of each fjord were similar to those at each fjord head, although the differences in salinity (higher in YF than PF) and ISM concentrations (higher in PF than YF) were clearer. Stations close to the fjord mouths were more influenced by the Beagle Channel. Thus, they were more similar between them but still presented some characteristics from each fjord.

3.2. Copepod abundance

Copepod community composition in both fjords was dominated by calanoid copepods. Five calanoid (*Clausocalanus bevipes, Ctenocalanus citer, Drepanopus forcipatus, Microcalanus pygmeaus, Paracalanus parvus*) and one cyclopoid (*Oithona* sp.) species represented more than 80% of the total copepod abundance (Fig. 3). Slightly lower abundances were observed in YF, where copepod abundances increased from the head (100 ind. m^{-3}) to the mouth of the fjord (780 ind. m^{-3}) (Fig. 4). On the contrary, PF showed the opposite trend: abundances were lower at the fjord mouth (653 ind. m^{-3}) than at stations influenced by melting icebergs (1100 ind. m^{-3}). Almost all the dominant species as well as some less abundant ones (e.g., *Chiridius glacialis Calanus simillimus, Oncaea* sp., *Calanus australis, Scolecithricidae minor*, *Metridia lucens*) showed higher abundances at stations with higher Chl-a concentrations, mostly located inside PF (Fig. 5a). Thus, copepod abundances in both fjords were mainly related to Chl-a concentrations, which explained 52% of the variance (Fig. 5b), whereas ISM, salinity, and the interaction of all three variables (i.e., salinity, ISM, Chl-a concentrations) accounted for only < 10% of the variance (Fig. 5b). The least abundant species (*Acartia tonsa, Scolecithricidae dentata, Calocalanus pavoninus*) comprised only 0.23 ± 0.07% of the total copepod abundance and were mostly related to higher salinities (Fig. 5a). Interestingly, only *Microcalanus pygmaeus* showed higher abundances with high loads of ISM (Fig. 5a).

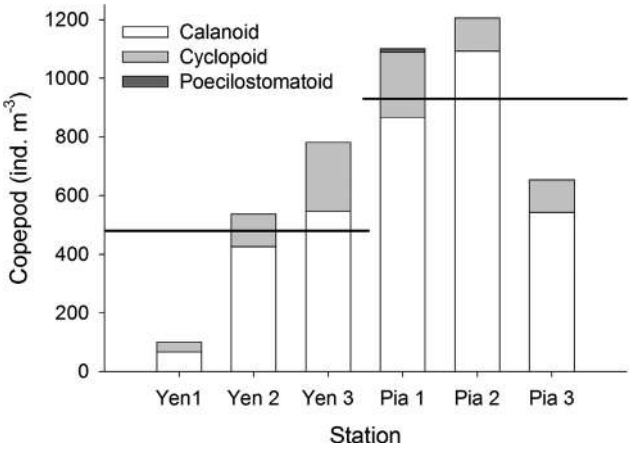

Fig. 4. Copepod abundance (ind. m^{-3}) in the water column along Yendegaia and Pia fjords. Horizontal black lines indicate the average abundance of total copepods for each fjord.

3.3. Copepod carcasses in the water column

The overall percentage of dead copepods collected in both fjords ranged from 10% at the middle of YF to 24% at the mouth of PF. Thus, the two fjords showed contrasting patterns. YF had the highest percentage of carcasses (19%) close to the river discharge (Yen 1), decreasing to almost half at the middle of the fjord, whereas PF showed increasing copepod carcasses from the head of the fjord (13%) to the middle (21%) and the fjord mouth (24%) (Fig. 6). Unfortunately, a problem with mortality in the sample collected at station 3 in YF made it impossible to distinguish between dead and living copepods.

In general, percentages of dead organisms were lower for small versus large copepods (Fig. 7). Mid-sized copepods (0.6–1 mm PL) such as *Microcalanus pygmaeus, Paracalanus parvus*, and *Clausocalanus brevipes* showed the lowest presence of dead individuals (7–12%) in both fjords, whereas the response of the small copepod, *Oithona* sp. (0.4 mm PL), differed depending on the fjord. Copepod mortality was highest for *Oithona* sp. in PF (32%), but remained close to the percentage registered for small copepods (13%) in YF. The percentage of dead individuals of the large copepod, *Depanopus forcipatus*, was similar in both fjords (20 and 22% in YF and PF, respectively). However, large abundances of

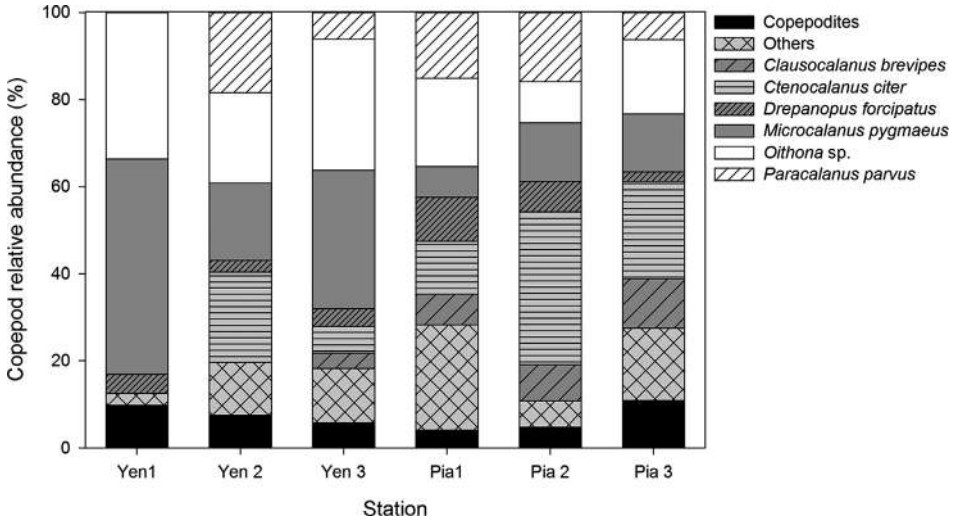

Fig. 3. Relative abundance of dominant copepod species in the water column in both fjords (Pia and Yendegaia) collected during October 2016.

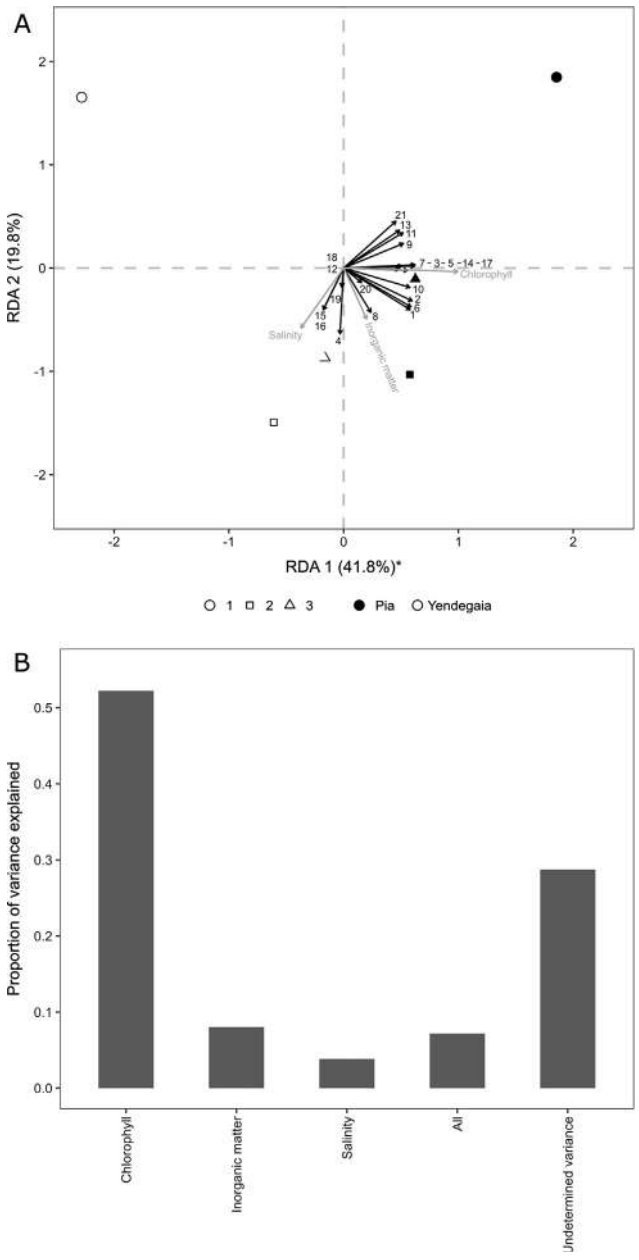

Fig. 5. Effects of chlorophyll, inorganic matter, and salinity on copepod abundances. (A) Redundancy analysis ordination for taxon abundances (logarithmically transformed) constrained by three independent variables. In the RDA correlation biplot, angles among response variables (black arrows) and explanatory variables (grey arrows), and among response variables or explanatory variables themselves, reflect their correlations. Points represent stations and coding by fjord (color) and station (symbols). The percentage of the variance explained by each axis in relation to the variance explained by RDA is given in brackets. Asterisks indicate marginal significant canonical axes (p value = 0.06). Species code: 1 Copepodites, 2 *Paracalanus parvus*, 3 *Clausocalanus brevipes*, 4 *Clausocalanus ingens*, 5 *Clausocalanus laticeps*, 6 *Ctenocalanus citer*, 7 *Drepanopus forcipatus*, 8 *Microcalanus pygmaeus*, 9 *Scolecithricidae minor*, 10 *Oithona* sp., 11 *Chiridius glacialis*, 12 *Candacia norvergica*, 13 *Calanus australis*, 14 *Calanus simillimus*, 15 *Calocalanus pavoninus*, 16 *Acartia tonsa*, 17 *Metridia lucens*, 18 *Scolecithricidae curtus*, 19 *Scolecithricidae dentata*, 20 *Spinocalanidae*, and 21 *Oncaea* sp. (B) Schematic bar plot of variance partitioning according to three explanatory variables: chlorophyll concentration, inorganic suspended matter concentration, and salinity.

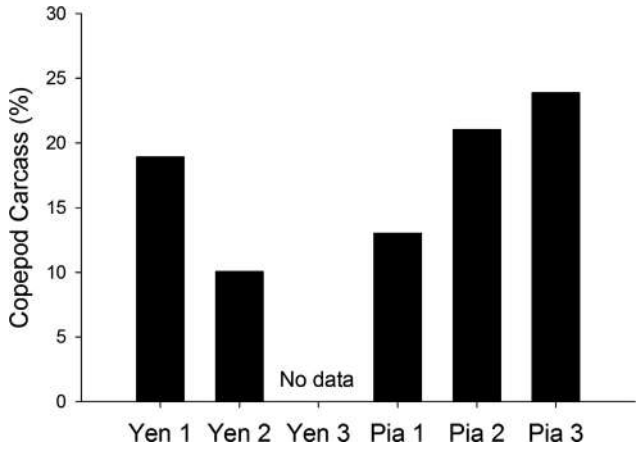

Fig. 6. Percentage of total copepod carcasses collected along the water column in the fjords Yendegaia and Pia during October 2016.

Chiridius sp., the largest copepod, only occurred in YF, where 24% of the population was found dead. The presence of carcasses belonging to unidentified copepodites was twice as high in YF (18%) as in PF (9%) (Fig. 7).

The presence of copepod carcasses in both fjords is better explained by the concentration of ISM rather than salinity (AICc = 0.92, Table 1). Copepod mortality was directly and strongly related to ISM ($R^2 = 0.74$; $p = 0.039$, $n = 5$); however, low salinities seemed to have only a weak effect on mortality ($R^2 = 0.32$; $p = 0.189$, $n = 5$; Fig. 8). No significant correlation was found between the percentage of dead copepods and temperature, organic seston, and Chl-a concentrations (data not shown).

3.4. Sediment traps

Vertical carbon fluxes (excluding swimmers and carcasses) at 50 m depth varied considerably between fjords. YF presented a maximum vertical carbon flux at the head of the fjord (390 mg C m^{-2} d^{-1}) that decreased to 236 mg C m^{-2} d^{-1} close to fjord mouth. PF had the opposite trend, with lower POC fluxes under melting icebergs (300 mg C m^{-2} d^{-1}) and twice these rates at the fjord mouth (595 mg C m^{-2} d^{-1}) (Fig. 9). The molar ratio (C:N) in YF varied widely between the fjord head (11) and mouth (3), whereas PF showed less variability from the head (5.7) to the mouth (8.3) (Table 2).

YF: The vertical flux of swimmers was higher at this fjord's head, with 10323 copepods m^{-2} d^{-1}, equivalent to 21% of the total POC flux (26% PON flux), whereas carcasses represented only 15% of the total copepods found in sediment traps, contributing a daily flux of 1857 copepods m^{-2} d^{-1}, or 3.4% and 4.1% of POC and PON fluxes, respectively. The percentage of dead copepods retained by sediment traps was similar at this fjord's mouth (14%), whereas the magnitude of the flux was almost half, with 5042 swimmers m^{-2} d^{-1} (5.8% of POC and 2.3% of PON fluxes) and 840 copepod carcasses m^{-2} d^{-1} (1% of POC and 0.4% of PON fluxes).

PF: Copepod abundances and percentages of dead copepods in the water column were the highest in this fjord (24 ± 3%), but the contributions of swimmers and carcasses to vertical fluxes were the lowest. The daily flux of swimmers (400 m^{-2} d^{-1}) contributed 1.4% of the POC flux (1% PON), and the carcasses (266 m^{-2} d^{-1}) contributed 1% of the POC flux (0.7% PON) at the fjord head. At PF mouth, there was a substantial increase in copepod abundance inside sediment traps, with fluxes of swimmers reaching 7,138 copepods m^{-2} d^{-1} and of carcasses reaching 2,508 m^{-2} d^{-1} (26% of carcasses). Swimmers contributed 7.2% of the POC flux (7.5% of the PON) and carcasses contributed 2.8% and 2.9% of POC and PON fluxes, respectively (Table 2).

Most larger calanoid copepod species (0.85–2.1 mm PL) collected

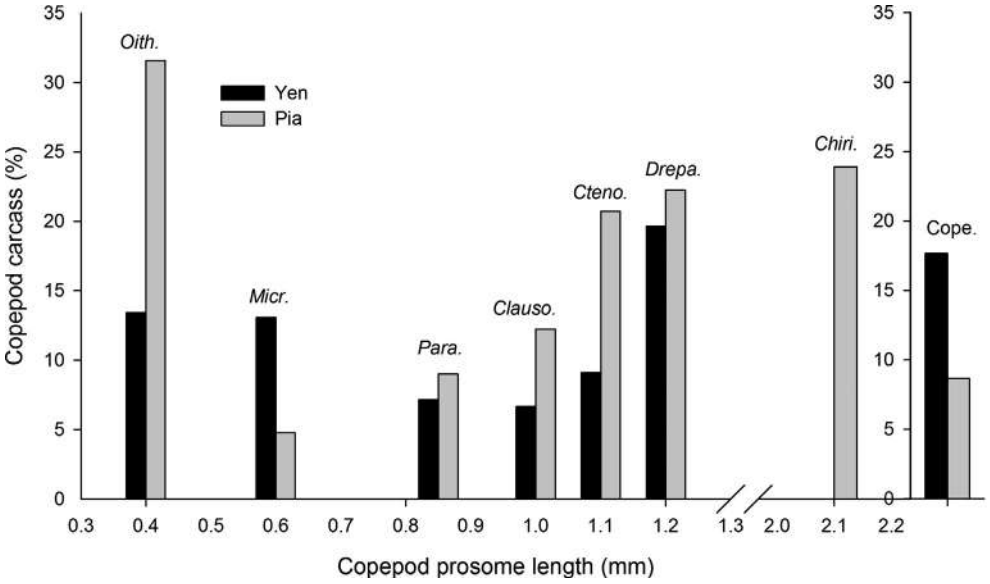

Fig. 7. Percentage of copepod carcasses of the most abundant copepod species collected along the water column in Yendegaia and Pia fjords during October 2016. Abbreviations of genus/specie names *Oith.* (*Oithona* sp.), *Micr.* (*Microcalanus pygmaeus*), *Para.* (*Paracalanus parvus*), *Clauso.* (*Calocalanus* spp.), *Cteno.* (*Ctenocalanus citer*), *Drepa.* (*Drepanopus forcipatus*), *Chiri.* (*Chiridius glacialis*), Cope. (unidentified copepodites).

Table 1
Model selection for the linear regression models fitted to copepod mortality (arcsine√deadcopepods %) and both environmental stressors potentially causing copepod mortality (i.e., inorganic suspended matter and salinity). The best-fitting model, according to second-order Akaike Information Criterion (AICc), is highlighted in bold. The table also shows the difference in AICc between both models (Delta AICc), the relative weight of each model (AICc Wt), and the cumulative weight of the models (Cum Wt).

Model	AICc	Delta AICc	AICc Wt	Cum Wt
Inorganic	9.36	0.00	0.92	0.92
Salinity	14.18	4.82	0.08	1.00

inside sediment traps were predominantly active swimmers, whereas small copepods (e.g., *Oncaea* sp., *Microcalanus pygmaeus*, *Oithona* sp.; < 0.8 mm PL) were mostly found dead (i.e., few swimmers occurred) (Fig. 10).

4. Discussion

4.1. Copepod mortality and community structure

The copepod species assemblages found in PF and YF are typical of the sub-Antarctic (SA) region (Fernández-Severini and Hoffmeyer, 2005). The dominance of *Oithona* sp., *Ctenocalanus citer*, *Clausocalanus brevipes*, and *Drepanopus forcipatus* in southern Patagonian fjords was consistent with other SA studies (Fernández-Severini and Hoffmeyer, 2005; Zagami et al., 2011; Aguirre et al., 2012; Biancalana et al., 2012). *Paracalanus parvus* is not a very common copepod in southern Patagonia channels (Beagle Channel Magellan Strait), being mainly restricted to fjords and small embayments in southern Patagonia, especially during late autumn (Biancalana et al., 2012). On the other hand, *Acartia tonsa* is usually a common inhabitant of fjords and channels, with high abundances in late summer and late spring in Ushuaia Bay (Biancalana et al., 2012), but decreasing numbers in late winter, which might explain the low densities found in PF and YF during October.

Both fjords have a similar orientation (N-S, N-E), their mouths are open to the Beagle Channel, and they are only 70 km apart. However, they have very distinct physical water column structures and pelagic productivity. The shallow pycnocline, large influx of inorganic matter at depth, and larger phytoplankton and copepod biomass of PF (marine-terminating glaciers) agree with previous findings on fjords with marine-terminating glaciers (Meire et al., 2017), where high productivity is promoted by episodic rise of nutrient-rich meltwater, upwelled close to the glacier bedrock. On the contrary, YF (land-terminating glaciers) shows a less stratified water column (Supplementary material Fig. 1), lower concentrations of particulate inorganic matter (mainly restricted to the upper 20 cm of the water column), and very low phytoplankton biomass and copepod abundances (especially at the station closest to the melt water influx). The low phytoplankton biomass in fjords with land-terminating glaciers (e.g., YF) is probably because meltwater is mainly transported in a very thin surface current at the fjord head (Fig. 2). This “glacier river plume” vanishes rapidly as it contacts brackish and marine waters. Mineral particles from river discharges are known to flocculate and aggregate in contact with sea water, increasing their size and sinking rates (Syvitski and Murray, 1981). Thus, most particles will settle close to the fjord head but only a small fraction are transported within the thin surface plume towards the fjord mouth as seen in YF. The effect of this process is a murky plume in only a very shallow layer; the rest of the water column remains transparent.

Copepods must cope with several environmental stressors distributed along horizontal and vertical dimensions in both fjords. In YF, copepods are most likely subjected to a bottom-up population control due to low phytoplankton biomass, which is probably related to restricted light penetration associated with the low transmittance observed in the upper water column (Fig. 2). High percentages of carcasses (24%) were only observed at the fjord head, where salinities were lower and concentrations of inorganic suspended matter higher (Fig. 8). Towards the fjord mouth, transmittance below 20 cm depth was > 91%, with low ISM and stable salinity and temperature throughout the water column. This coincides with the lowest presence of carcasses (13%). PF presented up to 50 times more Chl-a biomass than YF, having higher copepod abundances and displaying the highest percentage of dead copepods, closely coupled to high concentrations of ISM along the entire water column.

The effects of increasing sediment concentrations in the water column have been shown to affect important physiological processes in some calanoid copepods, such as reducing food uptake and egg production (Arendt et al., 2011). However, this is the first time that *in situ* mortality is observed in relation to ISM in the water column. Most studies have researched the osmotic effects of freshwater on copepod survival, which may cause significant reduction of some species, affecting community structure as observed in most fjords and estuaries around the world (Calliari et al., 2008; Elliott and Tang, 2011a,b; Giesecke et al., 2017). In those cases, there is a significant positive

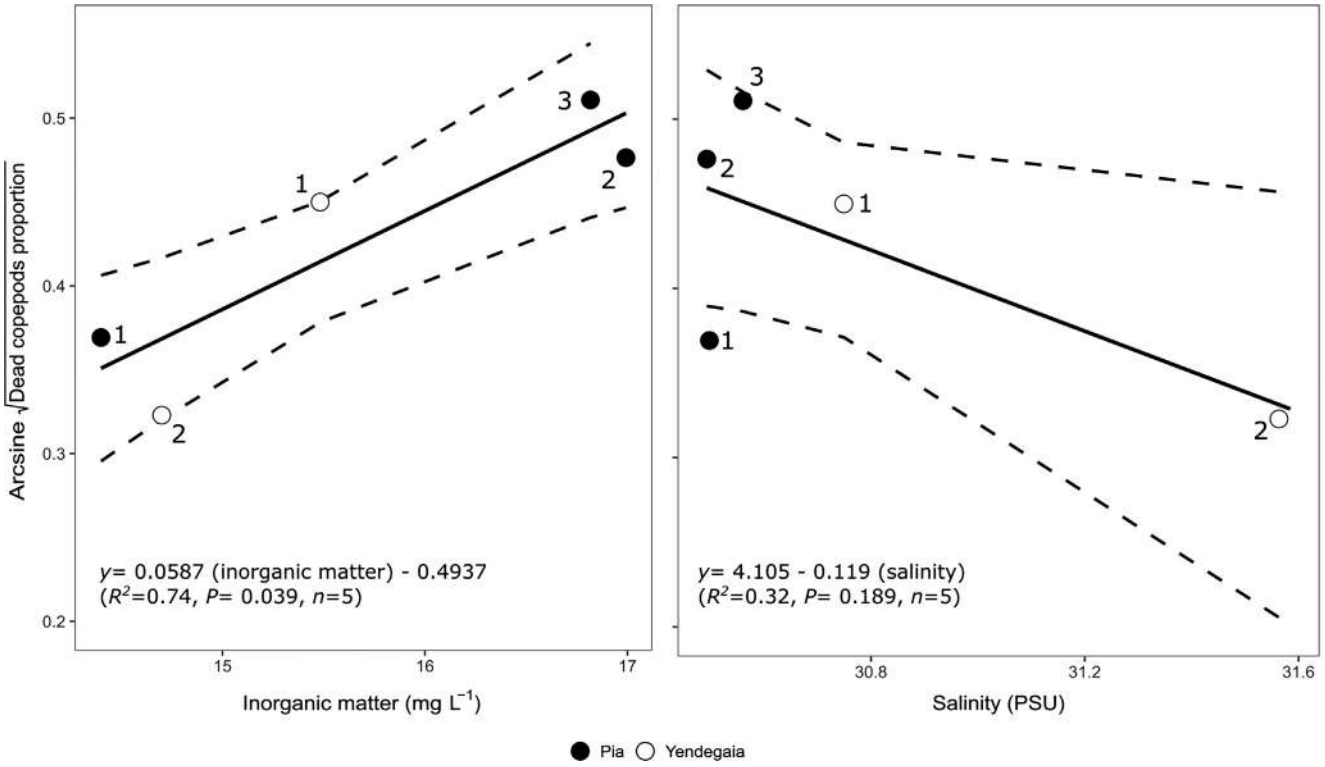

Fig. 8. Relationship between the percentage of total copepod carcasses and the most important environmental stressors (average salinity, concentration of inorganic suspended matter) recorded in the water column along the studied fjords during October 2016. Black dots indicate stations sampled inside Pia Fjord, whereas white circles represent stations sampled within Yendegaia Fjord.

selection towards eurihaline species (e.g., *Acartia tonsa*), which tend to dominate in those environments (Tester and Turner, 1991; Chaalali et al., 2013). The mortality of zooplankton organisms in relation to the amount of ISM has been observed for Antarctic krill (Fuentes et al., 2016), salps (Pakhomov et al., 2003), and under laboratory conditions for copepods (Arendt et al., 2011; Tang et al., 2011; Carrasco et al., 2013). Such mortality disrupts feeding, clogs particle collection systems, and causes overall physiological malfunctioning which leads to decreased growth, reproduction, and survival.

In this study, the effect of ISM is particularly variable among species and copepod sizes. Larger species tend to display the highest percentage of carcasses in these fjords (21–25%), whereas medium and small species tend to present fewer carcasses (5–14%). If this selective mortality pattern is preserved throughout the year, we would expect positive selective pressure over smaller copepods in fjords with high ISM, such as those having marine-terminating glaciers (i.e., PF). This agrees with the abundance pattern shown by the small *Microcalanus pygmaeus*: its highest abundances and lowest proportions of carcasses (5%) occur in environments with high ISM concentrations. The ability of this species to cope with high loads of suspended matter might depend on its feeding strategy. As observed by Michels and Schnack-Schiel (2005), this small copepod is most likely a raptorial predator rather than a filter-feeder as previously thought (Hopkins and Torres, 1989). Therefore, the presence of suspended materials would not significantly affect its feeding strategy.

On the contrary, the rest of the dominant copepods were all filter feeders such as *Paracalanus parvus* (Paffenhöfer et al., 1982) and *Ctenocalanus citer* (Michels and Schnack-Schiel, 2005), or had a gnatobase morphology that suggested phytoplankton was their main food source i.e., *Drepanopus forcipatus* (Hulsemann, 1985), *Chiridius glacilis*

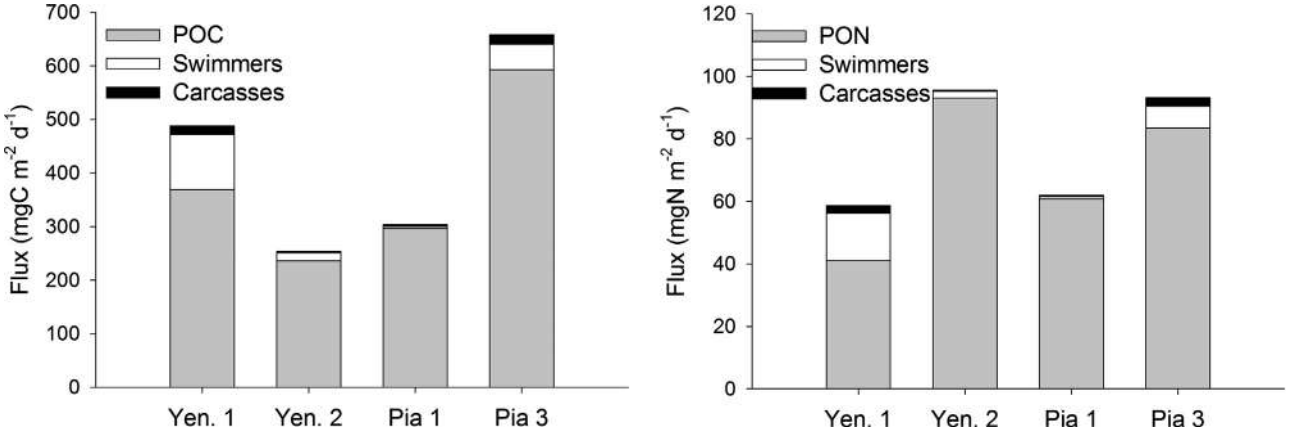

Fig. 9. Fluxes of carbon (left) and nitrogen (right) due to swimmers, carcasses, and total particulate organic carbon (left) and total particulate nitrogen collected by the sediment traps deployed inside Yendegaia and Pia fjords during October 2016.

Table 2
Contribution of carcasses and swimmers to the total carbon and nitrogen export at 50 m depth in the fjords Yendegaia and Pia during October 2016.

Station	Total C flux (mg C m^{-2} d^{-1})	Total N flux (mg N m^{-2} d^{-1})	C:N	Swimmers (cop. m^{-2} d^{-1})	Carcasses (cop. m^{-2} d^{-1})	Carcass flux (mg C m^{-2} d^{-1})	Swimmer flux (mg C m^{-2} d^{-1})	Carcass N flux (mg N m^{-2} d^{-1})	Swimmer N flux (mg N m^{-2} d^{-1})	Contribution of carcasses to total C flux (%)	Contribution of swimmers to total C flux (%)	Contribution of carcasses to total N flux (%)	Contribution of swimmers to total N flux (%)
Yen. 1	368.8 (28)	41.1 (4.6)	10.5	10323	1858	16.5	102.9	2.4	15.1	3.4	21.1	4.1	25.8
Yen. 2	236.2 (29.1)	93.1 (21.1)	3.0	5042	840	2.5	14.8	0.4	2.2	1.0	5.9	0.4	2.3
Pia 1	296.5 (52.9)	60.9 (17.5)	5.7	399	266	3.1	4.2	0.5	0.6	1.0	1.4	0.7	1
Pia 3	592.7 (27.5)	83.5 (2.8)	8.3	7138	2508	18.4	47.5	2.7	7.0	2.8	7.2	2.9	7.5

(Markhaseva, 1996), and *Clausocalanus brevipes* (Bradford-Grieve, 1999). This pattern suggests that these species might be further affected by clogging of filters and/or the unintentional ingestion of large concentrations of inorganic particles (i.e., minerals, clays), reducing their feeding efficiency, causing physiological damage and death of organisms such as the ones observed in PF. The higher proportion of carcasses showed by larger organisms might be related to their inability to do a proper selection of the particles ingested when exposed to high SIM. It has being observed that on filter feeders, the minimum food size does not change with body size; however its maximum food size limit increases with increasing copepod size (Wilson, 1973). Thus, larger organisms tend to be more generalist, and selection of particles becomes more difficult, especially in environments such as these with high loads of sediments, which would interfere in the capture of nutritious particles. This agrees with diet models which predict that selection against low quality food should be weaker when high quality food is scarce and stronger when high quality food is abundant (Lehman, 1976). Well feed individuals can afford the costs of selectivity, while poorly fed individuals will tend to decrease selectivity (DeMott, 1995). Both, selective grasping and nonselective filtering operate in a filter feeder (Richman and Rogers, 1969), thus, part of the time it will be using its filtering mode (taking particles within its capture size range), while part of the time it will select within a more narrow size range close to their optimum. The high proportion of SIM in relation to edible particles would increase handling time, reducing the feeding capacity and ultimately the viability of certain species in this kind of environments. In order unveil this mechanism, a more accurate identification of the proportion of dead copepodites stage of each species would be needed.

The overall percentage of *in situ* carcasses recorded in this study (13–27%) concurs with previous findings for estuaries (9–55%; Tang et al., 2006; Elliott and Tang, 2011b; Martínez et al., 2014; Giesecke et al., 2017) and is slightly higher than the mortality registered in coastal environments with lower abiotic stressors (< 20%; Yáñez et al., 2012). Therefore, these new findings imply that, in ecosystems with strong abiotic stress, non-predatory mortality may cause at least one third of copepod deaths.

4.2. Vertical fluxes

The contribution of carcasses in sediment traps is usually neglected in field studies due to the difficulty in discriminating between swimmers and carcasses. Thus, most studies usually screen the samples to exclude zooplankton from the vertical carbon flux registered by sediment traps (Buesseler et al., 2007). The identification of copepod carcasses using neutral red has being recently addressed by Ivory et al. (2014). They were able to obtain high levels of accuracy with this methodology when used in short deployments (24 h) with non-poisoned sediment trap samples. This affords a new opportunity for establishing the role that zooplankton carcasses play in the vertical carbon export in a variety of marine systems.

The total vertical carbon flux in this study (236–592 mgC m^{-2} d^{-1}) was slightly above the average recorded along Patagonian fjords, and significantly higher than the total flux measured in the Magellan Region using the same sediment traps at the same depths in northern Patagonia (Reloncaví Fjord, 334–725 mgC m^{-2} d^{-1}; González et al., 2010); central Patagonia (Puyuhuapi Channel and Aysen Fjord, 168–266 mgC m^{-2} d^{-1}; González et al., 2011); and southern Patagonia (Magellan Region, 73 mg C m^{-2} d^{-1}; González et al., 2016). The main components of the vertical carbon flux of these Patagonian fjords are usually fecal pellets (mainly from *Euphausia valentini* and copepods) and phytodetritus aggregates (González et al., 2011, 2016), with a C:N ratio close to the Redfield ratio or higher (i.e., C:N of 15; González et al., 2013).

Our measurements suggest that the particles settling at the head of YF are depleted in nitrogen, probably due to carbon-rich terrestrial organic inputs from the river, whereas at the YF mouth, the organic

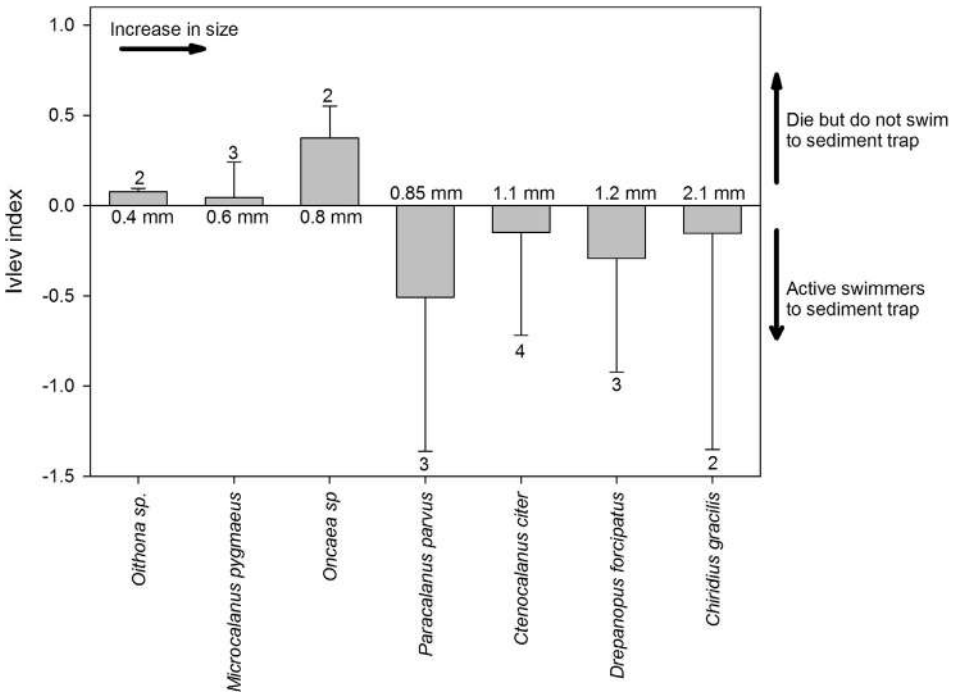

Fig. 10. Adapted version of Ivlev selectivity index. Index average (standard error) of most abundant copepod swimmers and carcasses collected by sediment traps. Values above 0 indicate that copepods were found in larger proportions as carcasses in sediment traps, whereas negative values indicate that copepods were found in larger proportions as swimmers. Numbers above the bars indicate the amount of sediment trap samples used to estimate the average.

matter was unexpectedly rich in nitrogen (C:N of 3), with a clear dominance of *Munida gregaria* pellets (unpublished results) that might have favored the colonization of nitrogen-rich microbes attached to the pellets (Fukami et al., 1981). This implies that sinking particles were a high-quality food source for the benthos in this fjord. PF, on the other hand, had a more stable C:N ratio (5.7–8.3) close to the Redfield ratio, indicating that the source of the exported organic matter is most likely from newly settling phytodetritus and fecal pellets, coincident with the higher phytoplankton biomass present in this fjord. The presence of carcasses in sediment traps did not make a significant contribution to the total particulate nitrogen or carbon fluxes as it was always < 4% of the total POC and < 3.4% of the PON, similar to the flux observed by Ivory et al. (2014). On the other hand, swimmers accounted for 1–21% of the total POC and 1–26% of the total PON. Thus, the exclusion of copepods from sediment trap samples when trying to estimate the export of POC seems to be justified, at least in short (days) and shallow (≈50 m depth) deployments.

The taxonomic composition of carcasses and swimmers differed in sediment traps. A negative trend in the applied selectivity index (adapted version of Ivlev index) was observed for larger copepods (> 0.85 mm PL). Thus, there are more large swimmers than carcasses in sediment traps. This is highly consistent with the ability of large copepods to migrate across greater vertical distances than small copepods, increasing the likelihood of the former entering sediment traps by chance. Smaller copepods (< 0.8 mm PL) were found in higher proportions as carcasses and less often as swimmers, meaning that these species settle downwards after dying in the upper water column (≈50 m depth), where they tend to spend most of their life. However, these results need to be taken with caution due to the few replicates (2–3) and high standard deviation of our estimates.

Copepod mortality is affected by natural stressors such as shifts in temperature, salinity, or low oxygen concentrations (Calliari et al., 2008; Elliott et al., 2010; Yáñez et al., 2012; Giesecke et al., 2017; Krautz et al., 2017). Here we have shown that apparently similar fjords with different geomorphologies present different environmental conditions (i.e., ISM, light penetration, food availability) that have different effects on the mortality of large and small copepods and, therefore, their contributions (as carcasses) to POC fluxes. This highlights the role of copepods as sentinels for the health of marine ecosystems.

Acknowledgments

This research was supported by the National Commission for Scientific and Technological Research (CONICYT) through project FONDAP-IDEAL, grant number 15150003. We would like to thank the captain and crew of the Forrest vessel for their professional assistant and help during sampling procedures.

Appendix A. Supplementary material

Supplementary data to this article can be found online at https://doi.org/10.1016/j.pocean.2018.10.011.

References

Aguirre, G.E., Capitanio, F.L., Lovrich, G.A., Esnal, G.B., 2012. Seasonal variability of metazooplankton in coastal sub-Antarctic waters (Beagle Channel). Mar. Biol. Res. 8 (4), 341–353.

Arendt, K.E., Dutz, J., Jónasdóttir, S.H., Jung-Madsen, S., Mortensen, J., Møller, E.F., Nielsen, T.G., 2011. Effects of suspended sediments on copepods feeding in a glacial influenced sub-Arctic fjord. J. Plankton Res. 33 (10), 1526–1537.

Arendt, K.E., Agersted, M.D., Sejr, M.K., Juul-Pedersen, T., 2016. Glacial meltwater influences on plankton community structure and the importance of top-down control (of primary production) in a NE Greenland fjord. Estuar. Coast. Shelf Sci. 183, 123–135. https://doi.org/10.1016/j.ecss.2016.08.026.

Ayata, S.D., Stolba, R., Comtet, T., Thiébaut, E., 2011. Meroplankton distribution and its relationship to coastal mesoscale hydrological structure in the northern Bay of Biscay (NE Atlantic). J. Plankton Res. 33, 1193–1211.

Banse, K., Falls, C.P., Hobson, L.A., 1963. A gravimetric method for determining suspended matter in sea water using Millipore filters. Deep-Sea Res. 10 (5), 639–642.

Bhatia, M.P., Kujawinski, E.B., Das, S.B., Breier, C.F., Henderson, P.B., Charette, M.A., 2013. Greenland meltwater as a significant and potentially bioavailable source of iron to the ocean. Nat. Geosci. 6, 274–278.

Biancalana, F., Diodato, S.L., Hoffmeyer, M.S., 2012. Seasonal and spatial variation of mesozooplankton biomass in Ushuaia and Golondrina Bays (Beagle Channel, Argentina). Braz. J. Oceanogr. 60 (1), 99–106.

Borcard, D., Legendre, P., Drapeau, P., 1992. Partialling out the spatial component of ecological variation. Ecology 73, 1045–1055.

Borcard, D., Gillet, F., Legendre, P., 2011. Canonical ordination. In: Borcard, D., Gillet, F., Legendre, P. (Eds.), Numerical Ecology with R. Springer, New York, pp. 153–226.

Bown, F., Rivera, A., Zenteno, P., Bravo, C., Cawkwell, F., 2014. First Glacier inventory and recent glacier variation on Isla Grande de Tierra del Fuego and adjacent islands in southern Chile. In: Global land ice measurements from space. Springer, Berlin Heidelberg, pp. 661–674.

Bradford-Grieve, J.M., 1999. The marine fauna of New Zealand: pelagic calanoid copepoda : *Megacalanidae*, *Calanidae*, *Paracalanidae*, *Mecynoceridae*, *Eucalanidae*,

Spinocalanidae, Clausocalanidae. New Zealand Oceanographic Institute memoir 0083-7903 102.
Buesseler, K.O., Antia, A.N., Chen, M., Fowler, S.W., Gardner, W.D., Gustafsson, Ö., Harada, K., Michaels, A.F., Rutgers, v.d., Loeff, M., Sarin, M., Steinberg, D.K., Trull, T., 2007. An assessment of the use of sediment traps for estimating upper ocean particle fluxes. J. Mar. Res. 65, 345–416.
Calliari, D., Borg, M.C.A., Thor, P., Gorokhova, E., Tiselius, P., 2008. Instantaneous salinityreductions affect the survival and feeding rates of the co-occurring copepods *Acartia tonsa* Dana and *A. clausi* Giesbrecht differently. J. Exp. Mar. Biol. Ecol. 362, 18–25.
Carrasco, N.K., Perissinotto, R., Jones, S., 2013. Turbidity effects on feeding and mortality of the copepod Acartiella natalensis (Connell and Grindley, 1974) in the St Lucia Estuary, South Africa. J. Exp. Mar. Biol. Ecol. 446, 45–51.
Chaalali, A., Beaugrand, G., Raybaud, V., Goberville, E., David, V., Boët, P., Sautour, B., 2013. Climatic facilitation of the colonization of an estuary by *Acartia tonsa*. PLoS One 8 (9), e74531.
Chu, V.W., 2014. Greenland ice sheet hydrology: a review. Prog. Phys. Geogr. 38 (1), 19–54.
Chu, V.W., Smith, L.C., Rennermalm, A.K., Forster, R.R., Box, J.E., Reeh, N., 2009. Sediment plume response to surface melting and supraglacial lake drainages on the Greenland Ice Sheet. J. Glaciol. 55, 1072–1082.
Core Team, R., 2012. R: A Language and Environment for Statistical Computing. R Foundation for Statistical Computing, Vienna, Austria.
Cuffey, K.M., Paterson, W.S.B., 2010. The Physics of Glaciers. Academic Press.
DeMott, W.R., 1995. Optimal foraging by a suspension-feeding copepod: responses to short-term and seasonal variation in food resources. Oecologia 103 (2), 230–240.
Dressel, D.M., Heinle, D.R., Grote, M.C., 1972. Vital staining to sort dead and live copepods. Chesapeake Sci. 13, 156–159.
Dyurgerov, M.B., Bring, A., Destouni, G., 2010. Integrated assessment of changes in freshwater inflow to the Arctic Ocean. J. Geophys. Res. 115 (D12), 1–9.
Elliott, D.T., Tang, K.W., 2009. Simple staining method for differentiating live and dead marine zooplankton in field samples. Limnol. Oceanogr. Methods 7, 585–594.
Elliott, D.T., Harris, C.K., Tang, K.W., 2010. Dead in the water: the fate of copepod carcasses in the York River estuary, Virginia. Limnol. Oceanogr. 55, 1821–1834.
Elliott, D.T., Tang, K.W., 2011a. Influence of carcass abundance on estimates of mortality and assessment of population dynamics in *Acartia tonsa*. Mar. Ecol. Prog. Ser. 427, 1–12.
Elliott, D.T., Tang, K.W., 2011b. Spatial and temporal distributions of live and dead copepods in the lower Chesapeake Bay (Virginia, USA). Estuaries Coasts 34, 1039–1048.
Fernández-Severini, M.D., Hoffmeyer, M.S., 2005. Mesozooplankton assemblages in two bays in the Beagle Channel (Argentina) during January 2001. Sci. Mar. 69 (S2), 27–37.
Fuentes, V., Alurralde, G., Meyer, B., Aguirre, G.E., Canepa, A., Wölfl, A.C., Hass, H.C., Williams, G.N., Schloss, I.R., 2016. Glacial melting: an overlooked threat to Antarctic krill. Sci. Rep. 6.
Fukami, K., Simidu, U., Taga, N., 1981. Fluctuation of the communities of heterotrophic bacteria during the decomposition process of phytoplankton. J. Exp. Mar. Biol. Ecol. 55, 171–184.
Giesecke, R., Vallejos, T., Sánchez, M., Teiguiel, K., 2017. Plankton dynamics and zooplankton carcasses in a mid-latitude estuary and their contributions to the local particulate organic carbon pool. Cont. Shelf Res. 132, 58–68.
González, H.E., Calderon, M.J., Castro, L., Clement, A., Cuevas, A., Daneri, G., Iriarte, J.L., Lizárraga, L., Martínez, R., Menschel, E., Silva, N., Carrasco, C., Valenzuela, C., Vargas, C.A., Molinet, C., 2010. Primary production and plankton dynamics in the Reloncaví Fjord and the Interior Sea of Chiloé, Northern Patagonia, Chile. Mar. Ecol. Prog. Ser. 402, 13–30.
González, H.E., Castro, L., Daneri, G., Iriarte, J.L., Silva, N., Vargas, C.A., Giesecke, R., Sánchez, N., 2011. Seasonal plankton variability in Chilean Patagonia fjords: Carbon flow through the pelagic food web of Aysen Fjord and plankton dynamics in the Moraleda Channel basin. Cont. Shelf Res. 31 (3–4), 225–243.
González, H.E., Castro, L.R., Daneri, G., Iriarte, J.L., Silva, N., Tapia, F., Teca, E., Vargas, C.A., 2013. Land–ocean gradient in haline stratification and its effects on plankton dynamics and trophic carbon fluxes in Chilean Patagonian fjords (47–50 S). Prog. Oceanogr. 119, 32–47.
González, H.E., Graeve, M., Kattner, G., Silva, N., Castro, L., Iriarte, J.L., Osman, L., Daneri, G., Vargas, C.A., 2016. Carbon flow through the pelagic food web in southern Chilean Patagonia: relevance of *Euphausia vallentini* as a key species. Mar. Ecol. Prog. Ser. 557, 91–110.
Hawkings, J.R., Wadham, J.L., Tranter, M., Lawson, E., Sole, A., Cowton, T., Tedstone, A.J., Bartholomew, I., Nienow, P., Chandler, D., Telling, J., 2015. The effect of warming climate on nutrient and solute export from the Greenland Ice Sheet. Geochem. Perspect. Lett. 1, 94–104.
Hopkins, T.L., Torres, J.J., 1989. Midwater food web in the vicinity of a marginal ice zone in the western Weddell Sea. Deep-Sea Res. I 36, 543–560.
Hulsemann, K., 1985. Two species of *Drepanopus* Brady (Copepoda Calanoida) with discrete ranges in the Southern Hemisphere. J. Plankton Res. 7 (6), 909–925.
Ivlev, V.S., 1961. Experimental Ecology of the Feeding of Fishes. Yale Univ. Press, New Haven, CT, USA, pp. 19–40.
Ivory, J.A., Tang, K.W., Takahashi, K., 2014. Use of Neutral Red in short-term sediment traps to distinguish between zooplankton swimmers and carcasses. Mar. Ecol. Prog. Ser. 505, 107–117.
Krautz, M.C., Hernández-Miranda, E., Veas, R., Bocaz, P., Riquelme, P., Quiñones, R.A., 2017. An estimate of the percentage of non-predatory dead variability in coastal zooplankton of the southern Humboldt Current System. Mar. Environ. Res. 132, 103–116.
Legendre, P., Legendre, L., 1998. Numerical Ecology. Elsevier Science B.V, Amsterdam.
Lehman, J.T., 1976. The filter-feeder as an optimal forager, and the predicted shapes of feeding curves. Limnol. Oceanogr. 21 (4), 501–516.
Markhaseva, E.L., 1996. Calanoid copepods of the family Aetideidae of the world ocean Russian Academy of Sciences, vol. 268, Zoological Institute.
Martínez, M., Espinosa, N., Calliari, D., 2014. Incidence of dead copepods and factors associated with non-predatory mortality in the Río de la Plata estuary. J. Plankton Res. 36 (1), 265–270.
McCune, B., 1997. Influence of noisy environmental data on canonical correspondence analysis. Ecology 78, 2617–2623.
Meire, L., Meire, P., Struyf, E., Krawczyk, D.W., Arendt, K.E., Yde, J.C., Juul Pedersen, T., Hopwood, M.J., Rysgaard, S., Meysman, F.J.R., 2016. High export of dissolved silica from the Greenland Ice Sheet. Geophys. Res. Lett. 43, 9173–9182.
Meire, L., Mortensen, J., Meire, P., Juul-Pedersen, T., Sejr, M.K., Rysgaard, S., Nygaard, R., Huybrechts, F., Meysman, F.J., 2017. Marine-terminating glaciers sustain high productivity in Greenland fjords. Glob. Change Biol. 23 (12), 5344–5357.
Michels, J., Schnack-Schiel, S.B., 2005. Feeding in dominant Antarctic copepods—does the morphology of the mandibular gnathobases relate to diet? Mar. Biol. 146 (3), 483–495.
Murray, C., Markager, S., Stedmon, C.A., Juul-Pedersen, T., Sejr, M.K., Bruhn, A., 2015. The influence of glacial melt water on bio-optical properties in two contrasting Greenlandic fjords. Estuar. Coast. Shelf Sci. 163, 72–83.
Paffenhöfer, G.-A., Stickler, J.r., Alcaraz, M., 1982. Suspension-feeding by herbivorous calanoid copepods: a cinematographic study. Mar. Biol. 67, 193–199.
Parsons, T.R., Maita, R., Lalli, C.M., 1984. Counting, Media and Preservation. A Manual of Chemical and Biological Methods for Seawater Analysis. Pergamon Press, Toronto.
Pakhomov, E.A., Fuentes, V., Schloss, I.R., Atencio, A., Esnal, G.B., 2003. Beaching of the tunicate *Salpa thompsoni* at high levels of suspended particulate matter in the Southern Ocean. Polar Biol. 26, 427–431.
Peres-Neto, P.R., Legendre, P., Dray, S., Borcard, D., 2006. Variation partitioning of species data matrices: estimation and comparison of fractions. Ecology 87, 2614–2625.
Richman, S., Rogers, J.N., 1969. The feeding of Calanus helgolandicus on synchronously growing populations of the marine diatom Ditylum brightwellii. Limnol. Oceanogr. 14 (5), 701–709.
Straneo, F., Curry, R.G., Sutherland, D.A., Hamilton, G.S., Cenedese, C., Våge, K., Stearns, L.A., 2011. Impact of fjord dynamics and glacial runoff on the circulation near Helheim Glacier. Nat. Geosci. 4 (5), 322.
Syvitski, J.P., Murray, J.W., 1981. Particle interaction in fjord suspended sediment. Mar. Geol. 39 (3–4), 215–242.
Tang, K.W., Freund, C.S., Schweitzer, C.L., 2006. Occurrence of copepod carcasses in the lower Chesapeake Bay and their decomposition by ambient microbes. Estuarine Coast. Shelf Sci. 68, 499–508.
Tang, K.W., Nielsen, T.G., Munk, P., Mortensen, J., Møller, E.F., Arendt, K.E., Tönnesson, K., Juul-pedersen, T., 2011. Metazooplankton community structure, feeding rate estimates, and hydrography in a meltwater-influenced Greenlandic fjord. Mar. Ecol. Prog. Ser. 434, 77–90. https://doi.org/10.3354/meps09188.
Tester, P., Turner, J., 1991. Why is *Acartia tonsa* restricted to estuarine habitats? Bull. Plankton Soc. Jpn. 1, 603–611.
Turner, J.T., 2002. Zooplankton faecal pellets, marine snow and sinking phytoplankton blooms. Aquat. Microb. Ecol. 27, 57–102.
Underwood, A.J., 1997. Experiments in Ecology. Cambridge University Press, Cambridge, UK.
Verity, P.G., Smetacek, V., 1996. Organism life cycles, predation, and the structure of marine pelagic ecosystems. Mar. Ecol. Prog. Ser. 277–293.
Wadham, J.L., Hawkings, J., Telling, J., Chandler, D., Alcock, J., O'Donnell, E., Kaur, P., Bagshaw, E., Tranter, M., Tedstone, A., Nienow, P., 2016. Sources, cycling and export of nitrogen on the Greenland Ice Sheet. Biogeosciences 13, 6339–6352.
Weydmann, A., Kwasniewski, S., 2008. Distribution of Calanus populations in a glaciated fjord in the Arctic (Hornsund, Spitsbergen) - The interplay between biological and physical factors. Polar Biol. https://doi.org/10.1007/s00300-008-0441-0.
Wilson, D.S., 1973. Food size selection among copepods. Ecology 54 (4), 909–914.
Yáñez, S., Hidalgo, P., Escribano, R., 2012. Mortalidad natural de *Paracalanus indicus* (Copepoda: Calanoida) en áreas de surgencia asociada a la zona de mínimo de oxígeno en el Sistema de Corrientes Humboldt: implicancias en el transporte pasivo del flujo de carbono. Revista de Biología Marina y Oceanografía 47 (2), 295–310.
Zagami, G., Antezana, T., Ferrari, I., Granata, A., Sitran, R., Minutoli, R., Guglielmo, L., 2011. Species diversity, spatial distribution, and assemblages of zooplankton within the Strait of Magellan in austral summer. Polar Biol. 34 (9), 1319–1333.